Applied Mathematical Modelling 35 (2011) 4304–4320

Contents lists available at ScienceDirect

Applied Mathematical Modelling

journal homepage: www.elsevier.com/locate/apm

Key design parameters and optimal design of a five-point double-toggle clamping mechanism

Ming-Shyan Huang *, Tsung-Yen Lin, Rong-Fong Fung

Department of Mechanical and Automation Engineering and Graduate Institute of Industrial Design, National Kaohsiung First University of Science and Technology, 2 Jhuoyue Rd., Nanzih, Kaohsiung City 811, Taiwan, ROC

ARTICLE INFO

Article history:
Received 7 February 2009
Received in revised form 21 February 2011
Accepted 2 March 2011
Available online 6 March 2011

Keywords:
Clamping unit
Five-point double-toggle clamping mechanism
Injection-molding machines
Genetic algorithm
GA

ABSTRACT

The toggle mechanism is highly efficient and yields excellent results; it is widely in the clamping units of injection-molding machines. This work explores the effect of key design parameters – the speed profile of the moving platen, the stroke of the clamping hydraulic cylinder and mold-opening, the ration of force amplification, and the initial angle of mold-closing on the performance of a five-point double-toggle clamping mechanism, drawing on a newly developed formulation of motion. The genetic algorithm (GA) is adopted to obtain the optimal solution of a clamping mechanism with reference to the key design parameters. Finally, the results of the primary mechanism are compared with those obtained using the optimal GA design and the GA design method is found to outperform the motion characteristics.

1. Introduction

An important feature of the toggle mechanism is its capacity to generate large forces at the slider with relatively low torque input. Burton [1] considered the toggle mechanism with hinge friction. Beer and Johnston [2] applied the principle of virtual work to analyze the toggle vise. In most cases, mechanisms that involve more than four links may be broken down into simple basic linkages and determined straightforwardly. The traditional toggle mechanism is a combination of two basic linkages, a four-bar mechanism and a slider-crank mechanism. The kinematic analysis of the entire toggle mechanism is conducted by considering the two basic linkages separately [3,4].

In recent years, most investigations of the design of toggle mechanisms have focused on mechanical advantages and ultimate stress under an external force. For example, Lin and Kuo [5] estimated the thrust required for the mold-clamping process of a five-point double-toggle clamping mechanism. Ignoring the inertia forces, they proposed a formula to estimate the thrust of the cross head mechanism in response to the clamping force. A parametric study demonstrated that the method was practicable and the individual profiles of the toggle linkages in the two mechanisms exhibited time saving characteristic, a large opening stroke, and/or thrust saving. Lin et al. [6] improved upon the stroke ratio and/or thrust saving of the conventional and Fanuc five-point double-toggle mould clamping mechanisms, based on the condition that the overall horizontal length cannot exceed the originally designed horizontal length in the investigation of Lin and Hsiao [7].

Fung et al. [8] employed both Hamilton's principle and Lagrange's multiplier method to derive an equation for the inertial force and the mechanism thrust. The Runge–Kutta integral method was implemented to analyze the kinematics and dynamics and compare them with those of the four-point and five-point toggle mechanisms. Fung et al. [9] also analyzed

* Corresponding author. Tel.: +886 7 6011000x2219; fax: +886 7 6011318.
E-mail address: mshuang@nkfust.edu.tw (M.-S. Huang).

0307-904X/$ - see front matter © 2011 Elsevier Inc. All rights reserved.
doi:10.1016/j.apm.2011.03.001

Notation

a	length of *Link a*
A	cross-section area of tie bars
A_m	stroke of mold-opened
A_X	coordinates of slider A in the x-axis
A_Y	coordinates of slider A in the y-axis
A_{xc}	positions of slider A at mold fully clamped
A_{xo}	positions of slider A at mold fully opened
b	length of the larger edge of *Crank O*
BP	barrier point
b_{max}	maximal stroke of the moving platen
c	length of the middle edge of *Crank O*
C_B	outer radius of Point B
C_{ji}	torque acting on the bearing
CL	central line
d	length of *Link d*
D_{xc}	positions of slider D at mold fully clamped
D_{xo}	positions of slider D at mold fully opened
e	distance between Point O and slider D
E	elastic modulus of tie bars
f	force exerted by the clamping hydraulic cylinder
f_{max}	maximal input force during clamping
F	force generated by the toggle mechanism
F_{ji}	force acting on the bearing
F_{jix}	sub-force of F_{ji} along the x-axis
F_{jiy}	sub-force of F_{ji} along the y-axis
F_M	ratio of force amplification
G_B	distance between outer radius of pin joint B and the CL
h	vertical distance between Points O and A
H_c	distance between Point O and CL
K_d	ratio of the stroke of mold-opening to that of the clamping hydraulic cylinder
K_d^*	desired value of the stroke ratio K_d
K_L	stiffness of the parallel links
K_M	stiffness of the mold
K_P	stiffness of the platen
K_S	total of stiffness of the stiffness K_T, K_M, K_P and K_L
K_T	stiffness of tie bars
K_v	ratio of the speed of the moving platen to that of the clamping hydraulic cylinder
Kv_{max}	local maximum in the Kv curve
Kv_{min}	local minimum in the Kv curve
l_1	a/b
l_2	c/b
l_3	d/b
L	length of tie bars
MA	mechanical advantage
n	number of tie bars
P_L	loss power caused by the frictions of pin joints
T_i	torque at the ith pin joint
V_A	speed of sliders A
V_D	speed of sliders D
R_A	radius pin joint A
R_B	radius pin joint B
R_C	radius pin joint C
R_D	radius pin joint D
R_{Kv}^*	desired ratio of Kv_{max} to Kv_{min}
R_O	radius pin joint O
ΔL	distance of elongated tie bars
α	angle between b and c
β	angle between *Link a* and horizontal line
ϕ_c	angle at mold fully clamped
ϕ_{fA}	angles of lines of action

ϕ_{fD}	angles of lines of action
ϕ_o	angle at mold fully opened
θ	angle between b and horizontal line
μ	coefficient of friction for all pin joints
μ_{jj}	coefficient of friction of member j on member i
ω_i	angular velocity of members i
ω_j	angular velocity of members j

the kinematics sensitivity of a newly designed toggle mechanism, which they treated as a combination of two slider-crank mechanisms, and exhibited excellent clamping efficiency.

The toggle mechanism is characterized by its mechanical advantages. The energy decreases if friction forces are present in the pin joints or lateral forces in the elastic links [10]. Additionally, the friction may produce heat or cause abrasion, and damage the bearings. To prevent the loss of mechanical advantage and to provide a sufficiently clamping force, a clamping force in excess of its theoretical value is typically required in practical design. To reduce the friction force, Fung et al. [11] proposed a new application of the toggle mechanism that is driven by a controlled permanent magnet and linear synchronous motor to replace the gears and other auxiliary mechanisms.

The toggle mechanism has the advantages of efficiency of motion and energy saving, and so is commonly adopted in a clamping mechanism in injection-molding machines. However, most studies [5–8] on the design of a toggle mechanism have focused on mechanical advantages and the ultimate stress under external forces. Neither motion performance nor production cost has been systematically considered in the design of a clamping mechanism using a simple genetic algorithm [12,13]. In this study, the following four important factors are considered: (1) the required quantity of strokes of the clamping hydraulic cylinder, (2) the initial speed of mold-closing, (3) the speed profile of the moving platen, and (4) the ratio of force amplification. The first item is associated with the machine length. The second and third items relate to the smoothness of motion and the lifetime of the machine, respectively. The final item concerns mechanical advantage. All of these factors are determined by the geometric dimensions of a toggle mechanism, and are considered in details in this work.

2. Key design parameters

Fig. 1 presents a typical toggle-type clamping unit of injection-molding machines. The part above the central line (*CL*) represents the toggle mechanism in a mold-closing state, and the part below the *CL* represents the toggle mechanism in a

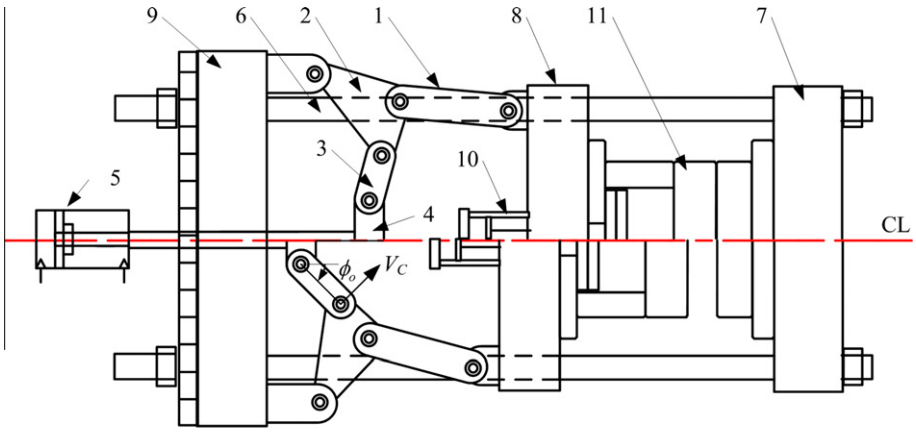

Item	Name	Item	Name
1	Moving platen side link (*Link a*)	7	Stationary platen
2	Rear platen side link (*Crank O*)	8	Moving platen
3	Cross head link (*Link d*)	9	Rear platen
4	Cross head	10	Ejection mechanism
5	Clamping hydraulic cylinder	11	Injection mold
6	Tie bar	CL	Central line

Fig. 1. Structure of a five-point double-toggle clamping mechanism.

maximal stroked mold-opening state. The clamping unit is responsible for the closing, opening and clamping of a mold and the ejection of the injected parts. Notably, to prevent molten plastics from flashing from the cavities during molding, the clamping mechanism must apply sufficient force, of approximately hundreds or even thousands of tons, to keep the mold closed. The clamping force is produced by the stretching of tie bars when the cross head is moved forward to its dead locked position, where *Link a* and *Crank O* are extended straight.

Not only must the mechanical advantage be maximized, favorable motion performance ensured and the production cost of clamping units for injection-molding machines kept low, but also various key parameters must be considered in the design of a toggle mechanism:

(1) *Speed profile of the moving platen.* Fig. 2 plots the typical speed profile of a moving platen in a five-point double-toggle clamping mechanism corresponding to its stroke. As the mold closes, a fast moving platen produces a large thrust and influences the smoothness of the motion of the moving platen. Minimizing the difference between the local minimum and the local maximum speeds helps to smooth the motion of the moving platen.
(2) *Strokes of clamping hydraulic cylinder and mold-opening.* The quantity of the stroke of mold-closing depends on the stroke of the cross head. In an efficient design of the mold-opening stroke, a shorter stroke of the clamping hydraulic cylinder leads to a longer mold-opening stroke, and the small dimensions of the machines keep the costs low.
(3) *Ratio of force amplification.* High force amplification, which is the ratio of the designed output force to the maximal input force of a clamping mechanism, is designed to enable a low input force to generate a high clamping force. If this high force amplification achieved, energy is saved and the production cost is reduced.
(4) *Initial angle of mold-closing.* Based on Fig. 1, the angle ϕ_o is defined as the initial angle from which the closed mold is fully opened. A larger initial angle ϕ_o corresponds to a larger horizontal component of velocity V_C, which pushes the *Crank O*.

The design of the toggle clamping mechanism must consider several important features, such as structural strength, framework vibration and lifetime of the clamping mechanism, among others. However, this work focuses only on the above four key design parameters and addresses their effects on the performance of the mechanism.

3. Governing equations

Before the importance of various key parameters to mechanical motion is discussed, the governing equations of the five-point double-toggle clamping mechanism are derived.

Fig. 3 presents the diagram of a five-point double-toggle clamping mechanism structure, where slider *D* represents the cross head; slider *A* represents the moving platen, and Point *O* is the pin joint which connects *Crank O* to the rear platen. The toggle mechanism comprises two sets of slider-crank mechanisms – the driving part, *DCO,* and the driven part, *OBA*. Point *O* is the origin of the coordinates, and the coordinates (A_X, A_Y) of slider *A* can be derived as,

$$A_X = b\cos\theta + a\cos\beta, \tag{1}$$

$$A_Y = b\sin\theta - a\sin\beta = h, \tag{2}$$

where *a* denotes the length of *Link a* and *b* is the length of the larger edge of *Crank O*. The term *h* in Eq. (2) represents the vertical distance between Points *O* and *A*, and must be sufficiently large to accommodate the ejection mechanism. However, a large *h* exerts a significant bending moment on the moving platen. Usually, *h* is set to allow the direction of motion of slider *A* to be in the same horizontal plane as the axes of the lower tie bars.

The speed V_A of slider *A* is derived by differentiating Eq. (1) with respect to time prior to Eq. (2) is substituted into Eq. (1):

$$V_A = -b(\sin\theta + \tan\beta\cos\theta)\,\dot{\theta}. \tag{3}$$

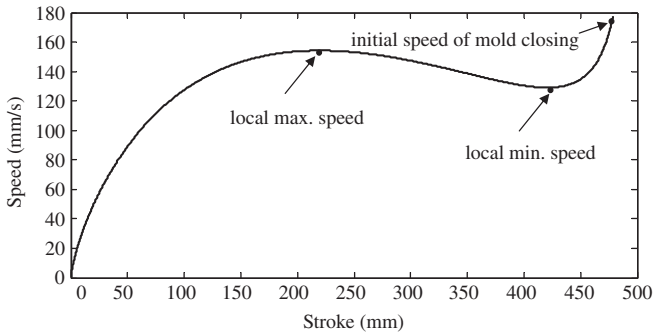

Fig. 2. Typical speed profile versus stroke of moving platen in a five-point toggle clamping mechanism.

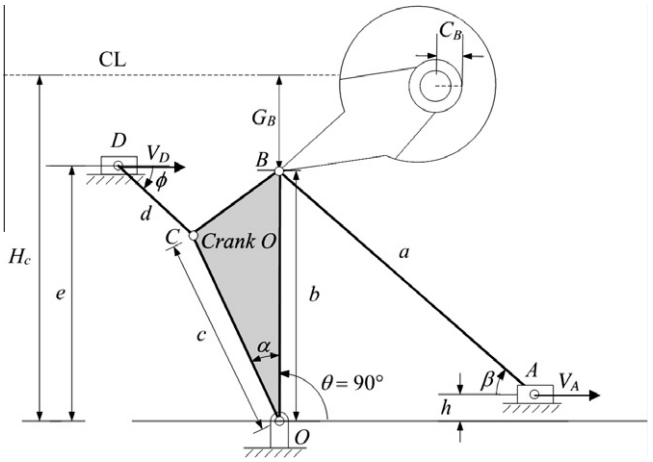

Fig. 3. Five-point double-toggle clamping mechanism.

The driving part *DCO* is connected to a clamping hydraulic cylinder. Given that $\theta' = \alpha + \theta$ and the coordinates (D_X, D_Y) of slider *D* are described as,

$$D_x = c\cos\theta' - d\cos\phi, \tag{4}$$

$$D_Y = c\sin\theta' + d\sin\phi = e, \tag{5}$$

where *c* is the length of the middle edge of *Crank O*; *d* is the length of *Link d*, and *e* is the distance between Point *O* and slider *D*. The speed V_D of slider *D* is obtained by differentiating Eq. (4) with respect to time and then substituting Eq. (5) into Eq. (4):

$$V_D = -c(\sin\theta' + \tan\phi\cos\theta')\dot{\theta}. \tag{6}$$

In a typical five-point double-toggle clamping mechanism, the stroke of the clamping hydraulic cylinder directly affects the maximal mold-opening stroke. The ratio of the stroke of mold-opening to that of the clamping hydraulic cylinder is K_d, which is derived from Eqs. (1) and (4) as,

$$K_d = \frac{A_{xo} - A_{xc}}{D_{xo} - D_{xc}}, \tag{7}$$

where D_{xo} and D_{xc} represent the positions of slider *D* and A_{xo} and A_{xc} represent those of slider *A* when the mold is fully opened and clamped, respectively. K_d represents the efficiency of a toggle mechanism in providing a long mold-opening stroke.

The speed of the moving platen in a toggle mechanism is controlled by setting the clamping hydraulic cylinder speed. Dividing Eq. (3) by Eq. (6) yields

$$K_v = \frac{V_A}{V_D} = \frac{-b(\sin\theta + \tan\beta\cos\theta)}{-c(\sin\theta' + \tan\phi\cos\theta')}, \tag{8}$$

where K_v denotes the ratio of the speed of the moving platen to that of the clamping hydraulic cylinder.

4. Effects of friction on mechanical advantage

Notably, a five-point toggle clamping mechanism is adopted to exploit the generation of large output clamping force, which corresponds to a small input force. The ratio of output force to input force is the mechanical advantage. However, the friction effects in every joint and slider reduce the theoretical mechanical advantage. This work thus takes the effect of friction into account to calculate accurately the forces associated with the toggle mechanism. Fig. 4(a) demonstrates as an example a diagram of the force delivered between member *i* (link) and member *j* (bearing), where *r* represents the radius of the bearing. Based on the assumption that no tolerance exists between members *i* and *j*, the force with which member *j* acts on member *i*, called the bearing force, is F_{ji}, which has two sub-forces, F_{jix} and F_{jiy}, and a torque, C_{ji}, as displayed in Fig. 4(b). C_{ji} can be expressed as,

$$C_{ij} = r_\mu |F_{ji}| sign(\omega_j - \omega_i) \cong \mu r\sqrt{\left(F_{jix}^2 + F_{jiy}^2\right)} sign(\omega_j - \omega_i), \tag{9}$$

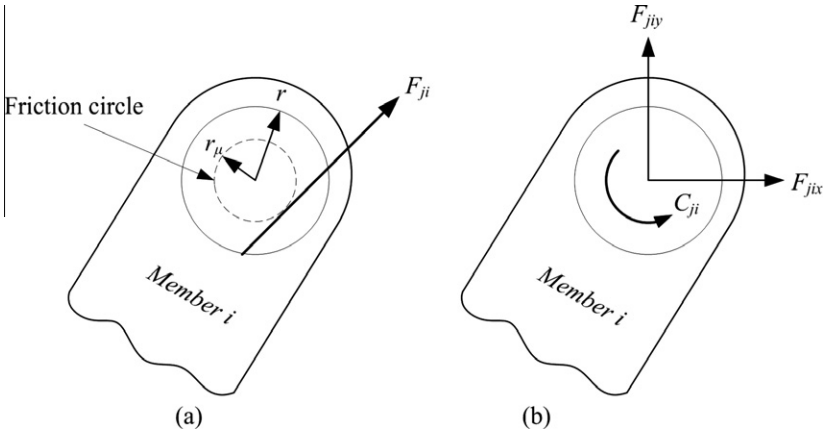

Fig. 4. Force delivery between link (Member *i*) and bearing (Member *j*).

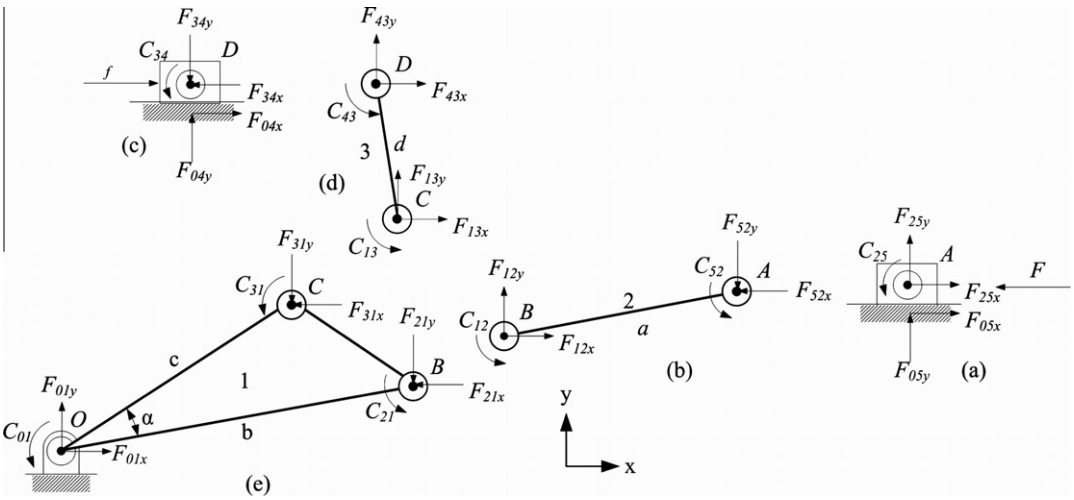

Fig. 5. Free body diagram of five-point double-toggle clamping mechanism.

where the *sign* function is defined as,

$$sign(\omega_j - \omega_i) = \begin{cases} -1 & \text{if} \quad (\omega_j - \omega_i) < 0 \\ 0 & \text{if} \quad (\omega_j - \omega_i) = 0 \\ +1 & \text{if} \quad (\omega_j - \omega_i) > 0, \end{cases} \tag{10}$$

where ω_i and ω_j represent the angular velocity of members *i* and *j*, respectively. The free body diagram in Fig. 4(b) is further applied to calculate the mechanical advantage, *MA*, as follows:

Fig. 5 presents the free body diagram of a five-point double-toggle clamping mechanism. The toggle mechanism comprises two sets of slider-crank mechanisms – the driving part *DCO* and the driven part *OBA*. The forces *F* and *f*, which are exerted on slider A and slider *D*, respectively, are a reaction force that resists the elongation of the tie bars and a thrust force that moves the cross head. Fig. 5(a) shows the free body diagram of slider *A*. The force equations for slider *A* are,

$$F_{03x} + F_{23x} = \mu_{03}|F_{03y}|sign(-\dot{S}_A) - F_{32x} = F, \tag{11a}$$

$$F_{03y} + F_{23y} = 0 = F_{03y} - F_{32y}, \tag{11b}$$

where $\dot{S}_A$ is the velocity of slider *A* and is positive to the right. When slider *A* moves to the right, $\dot{S}_A$ is positive and the friction force F_{03x} is negative. Then, the forces that act on connecting rod 2 and the moment at Point *B*, as presented in Fig. 5(b), are given by

$$F_{12x} + F_{32x} = 0, \tag{12a}$$

$$F_{12y} + F_{32y} = 0, \tag{12b}$$

$$F_{32y}acos\beta - F_{32x}asin\beta + \mu_{12}R_B(F_{12x}^2 + F_{12y}^2)^{1/2}sign(\omega_1 - \omega_2) + \mu_{32}R_A\left(F_{32x}^2 + F_{32y}^2\right)^{1/2}sign(\omega_3 - \omega_2) = 0. \tag{12c}$$

Solving Eqs. (12a) and (12b) for F_{12x} and F_{12y}, and then substituting the resulting expressions into Eq. (12c) yields,

$$F_{32y}a\cos\beta - F_{32x}a\sin\beta + K_A\sqrt{\left(F_{32x}^2 + F_{32y}^2\right)} = 0, \tag{13a}$$

$$K_A = \mu_{12}R_B sign(\omega_1 - \omega_2) + \mu_{32}R_A sign(\omega_3 - \omega_2). \tag{13b}$$

The angle ϕ_{fA} in Fig. 6(a) depends on whether the connecting rod is in tension or compression and whether C_{12} and C_{32} are clockwise or counterclockwise. That the value of ω_1–ω_2 is negative means that C_{12} is clockwise and C_{32} is counterclockwise. Expressing the force components F_{32x} and F_{32y} in terms of polar coordinates yields,

$$F_{32x} = F_{32}\cos\phi_{fA}, \tag{14a}$$

$$F_{32y} = F_{32}\sin\phi_{fA}. \tag{14b}$$

Substituting Eqs. (14a) and (14b) into Eq. (13a) yields the angle ϕ_{fA} angle as,

$$\phi_{fA} = \pi - \left[\sin^{-1}\left(-\frac{K_A}{a}\right) - \beta\right]. \tag{14c}$$

Combining Eqs. (11a) and (11b) yields,

$$\mu_{03}|F_{32y}|sign(\dot{S}_A) + F_{32x} + F = 0. \tag{14d}$$

Substituting Eqs. (14a) and (14b) into this equation yields

$$F_{32} = \frac{-F}{\mu_{03}|\sin\phi_{fA}|sign(\dot{S}A) + \cos\phi_{fA}}. \tag{14e}$$

The total forces exerted by slider D and rod 5, presented in Fig. 5(c) and (d), and the moment at Point C are induced as,

$$F_{56x} + F_{06x} = \mu_{06}|F_{06y}|sign(-\dot{S}_D) + F_{56x} = -f, \tag{15a}$$

$$F_{56y} + F_{06y} = 0 = -F_{56y} + F_{06y}, \tag{15b}$$

$$F_{65x} + F_{15x} = 0, \tag{16a}$$

$$F_{65y} + F_{15y} = 0, \tag{16b}$$

$$F_{65y}d\cos\phi + F_{65x}d\sin\phi - \mu_{15}R_C(F_{15x}^2 + F_{15y}^2)^{1/2}sign(\omega_1 - \omega_5) - \mu_{65}R_D\left(F_{65x}^2 + F_{65y}^2\right)^{1/2}sign(\omega_6 - \omega_5) = 0. \tag{16c}$$

F_{12x} and F_{12y} can be obtained using Eqs. (16a) and (16b). The values are substituted into Eq. (16c), yielding

$$F_{65y}d\cos\phi + F_{65x}d\sin\phi - K_D\sqrt{(F_{65x}^2 + F_{65y}^2)} = 0, \tag{17a}$$

$$K_D = \mu_{15}R_C sign(\omega_1 - \omega_5) + \mu_{65}R_D sign(\omega_6 - \omega_5). \tag{17b}$$

The ϕ_{fD} angle in Fig. 6(b) depends on whether the connecting rod is in tension or under compression and C_{15} and C_{65} are clockwise or counterclockwise. A negative value of ω_1–ω_5 means that both C_{15} and C_{65} are counterclockwise. The force components F_{65x} and F_{65y} in polar coordinates are,

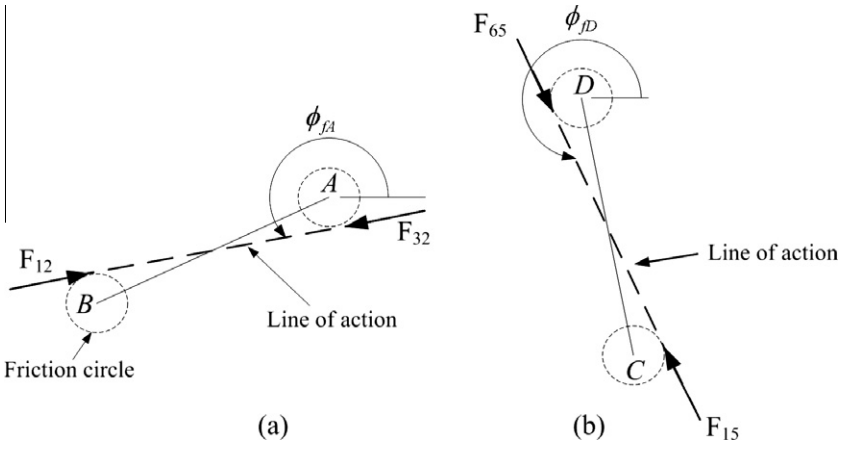

Fig. 6. Force that acts on bearings.

$$F_{65x} = F_{65}\cos\phi_{fD}, \tag{18a}$$
$$F_{65y} = F_{65}\sin\phi_{fD}. \tag{18b}$$

Substituting Eqs. (18a) and (18b) into Eq. (17a), yields the ϕ_{fD} angle as,

$$\phi_{fD} = -\left[\sin^{-1}\left(-\frac{K_D}{d}\right) - \phi\right]. \tag{18c}$$

Then, combining Eqs. (15a) with (15b) yields

$$\mu_{06}|F_{65y}|sign(\dot{S}_D) + F_{65x} + f = 0. \tag{18d}$$

Further, substituting Eqs. (18a) and (18b) into this equation yields

$$F_{65} = \frac{f}{\mu_{06}|\sin\phi_{fD}|sign(\dot{S}_D) + \cos\phi_{fD}}. \tag{18e}$$

The force components in the x- and y-direction are,

$$F_{32x} = -F_{23x} = -F_{12x} = F_{21x} = F_{32}\cos\phi_{fA}, \tag{19a}$$
$$F_{32y} = -F_{23y} = -F_{12y} = F_{21y} = F_{32}\sin\phi_{fA}, \tag{19b}$$
$$F_{65x} = -F_{56x} = -F_{15x} = F_{51x} = F_{65}\cos\phi_{fD}, \tag{19c}$$
$$F_{65y} = -F_{56y} = -F_{15y} = F_{51y} = F_{65}\sin\phi_{fD}. \tag{19d}$$

Once F_{21x}, F_{21y}, F_{51x} and F_{51y} have been determined, the analysis can be completed by solving the following equations, which specify the forces that act on crank 1.

$$F_{01x} + F_{21x} + F_{51x} = 0, \tag{20a}$$
$$F_{01y} + F_{21y} + F_{51y} = 0, \tag{20b}$$
$$C_{01} + C_{21} + C_{51} + F_{21y}b\cos\theta - F_{21x}b\sin\theta + F_{51y}c\cos(\alpha+\theta) - F_{51x}c\sin(\alpha+\theta) = 0, \tag{20c}$$
$$C_{01} = \mu_{01}R_O[(F_{01x} + F_{01x})^2]^{1/2}sign(\omega_0 - \omega_1), \tag{20d}$$
$$C_{21} = \mu_{21}R_B[(F_{21x} + F_{21x})^2]^{1/2}sign(\omega_2 - \omega_1), \tag{20e}$$
$$C_{51} = \mu_{51}R_C[(F_{51x} + F_{51x})^2]^{1/2}sign(\omega_5 - \omega_1). \tag{20f}$$

Finally, combine Eqs. (19a)–(19d), (20a)–(20f) to determine the instantaneous efficiency from the friction factor; the *MA* function is thus obtained:

$$MA = \frac{F}{f} = \frac{-K_4}{K_1} \pm \frac{\sqrt{(2K_4)^2 - 4K_1(\mu_{01}^2R_0^2 - K_3^2)}}{2K_1}K_5, \tag{21a}$$
$$K_1 = \mu_{01}^2R_0^2 - K_2^2, \tag{21b}$$
$$K_2 = \mu_{21}R_Bsign(\omega_2 - \omega_1) + b\sin(\phi_{fA} - \theta), \tag{21c}$$
$$K_3 = \mu_{51}R_Csign(\omega_5 - \omega_1) + c\sin(\phi_{fD} - \theta'), \tag{21d}$$
$$K_4 = \mu_{01}^2R_0^2\cos(\phi_{fA} - \phi_{fD}) - K_2K_3, \tag{21e}$$
$$K_5 = \frac{-\mu_{03}|\sin\phi_{fA}|sign(\dot{S}_A) + \cos\phi_{fA}}{\mu_{06}|\sin\phi_{fD}|sign(\dot{S}_D) + \cos\phi_{fD}}, \tag{21f}$$
$$\phi_{fA} = \pi - \left[\sin^{-1}\left(-\frac{K_A}{a}\right) - \beta\right], \tag{21g}$$
$$K_A = \mu_{12}R_Bsign(\omega_1 - \omega_2) + \mu_{32}R_Asign(\omega_3 - \omega_2), \tag{21h}$$
$$\phi_{fD} = -\left[\sin^{-1}\left(-\frac{K_D}{d}\right) - \phi\right], \tag{21i}$$
$$K_D = \mu_{15}R_Csign(\omega_1 - \omega_5) + \mu_{65}R_Dsign(\omega_6 - \omega_5), \tag{21j}$$

where f and F are the force exerted by the clamping hydraulic cylinder and the force generated by the toggle mechanism, respectively; μ_{jj} is the coefficient of friction of member j on member i, and is assumed to be the same for each pin joint; R_O, R_A, R_B, R_C and R_D are the radii of the five-point pin joints O, A, B, C and D, respectively. ϕ_{fA} and ϕ_{fD} are the angles of lines of action. The Appendix presents in detail the derivation of above equations. Eq. (21a) represents the force amplification ratio, called mechanical advantage, of a toggle mechanism, and is a nonlinear function that corresponds to the position of mold-closing.

5. Rigidity of mechanism and clamping force

Based on the assumption that components of the toggle clamping mechanism are all rigid bodies, the mechanism theoretically operates in the state of infinite mechanical advantage when *Link a* and *Crank O* are completely straightened. Restated, straightened rigid links will produce a reacting force that causes the clamping hydraulic cylinder to straighten them easily and then to generate a clamping force. In fact, the clamping force deforms both the links and the mold, and elongates the tie bars. Thus, before the straightening process, the clamping hydraulic cylinder must provide an extra force to overcome power loss in the deformations and elongations.

Based on the assumption that the stiffness K_S of the clamping mechanism represents the total of the stiffness K_T, K_M, K_P and K_L of the tie bars, mold, platen and parallel links, respectively, the force F that acts on moving platen is given by,

$$F = K_S \Delta L = \left(\frac{1}{K_T} + \frac{1}{K_M} + \frac{1}{K_P} + \frac{1}{K_L}\right)^{-1} \Delta L. \tag{22}$$

Since the tie bars are the least rigid parts of the clamping mechanism, the system stiffness K_S is approximated by

$$K_S \cong K_T = n\frac{AE}{L}, \tag{23}$$

where n, L, A and E are the number, length, area, and elastic modulus of the tie bars, respectively. In the clamping stage, the moving platen moves through a distance ΔL as the tie bars are elongated. The distance ΔL is expressed as:

$$\Delta L = A_{xc} - A_{xt}, \tag{24}$$

where A_{xc}, and A_{xt} are the positions of slider A at the fully clamped point and the initial point of mold-clamping. Hence, ΔL is the elongation of the tie bars. Fig. 7 presents the clamping force as a function of the elongation of tie bars in the clamping stage. When the mold is closed and then compressed, ΔL increases, such that the MA value increases. These changes are characteristics of a toggle mechanism: the force in the toggle mechanism that acts on the mold, F, increases immediately after the mold is closed and full clamping is required. Combining Eqs. 21a, 22, 23, and 24 yields the input force f:

$$f = \frac{F}{MA} = \frac{K_S \Delta L}{MA}. \tag{25}$$

In Fig. 7, the dashed line represents the force in response to the deformation by the toggle mechanism. The BP is the barrier point, which appears at the location of the maximal input force during clamping, f_{max}. Consequently, when the elongated tie bars passes over BP, the MA value increases greatly and the clamping hydraulic cylinder need not generate a larger input force than f_{max} to ensure that the mold is fully clamped. The force amplification ratio of F_M, the clamping force, to the maximal input force is defined as,

$$F_M = \frac{F}{f_{max}}. \tag{26}$$

6. Effect of key design parameters on mechanical performance

To design a five-point double-toggle clamping mechanism, the key parameters, such as the link lengths a, b, c, d, and the angles α and ϕ_c angles, presented in Fig. 3, are of utmost importance. ϕ_c is the value of ϕ in a fully clamped state. The length b

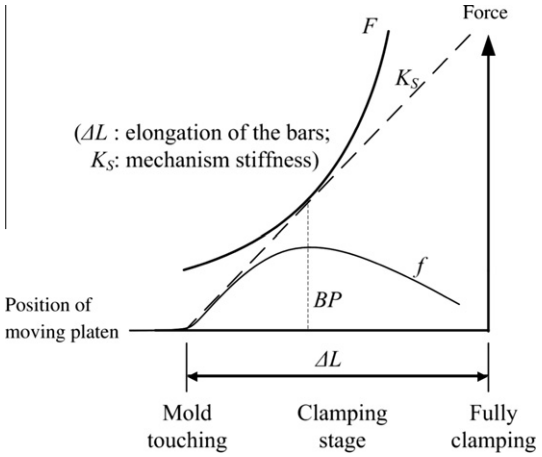

Fig. 7. Clamping force as a function of the elongation of tie bars.

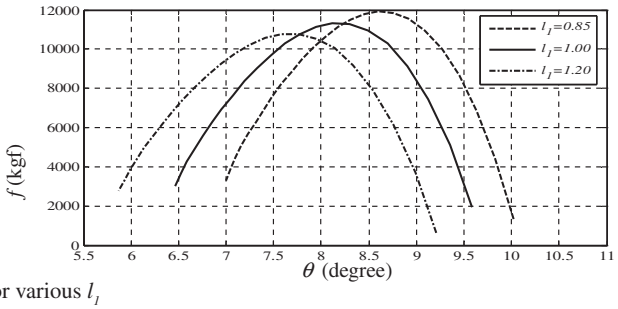

(a) for various l_1

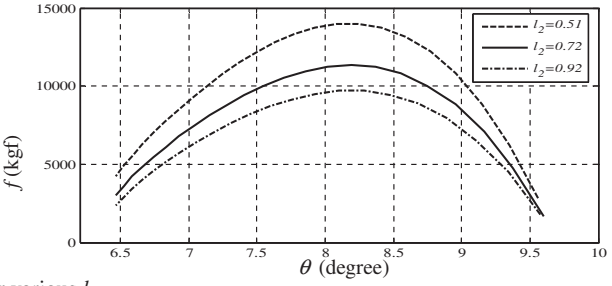

(b) for various l_2

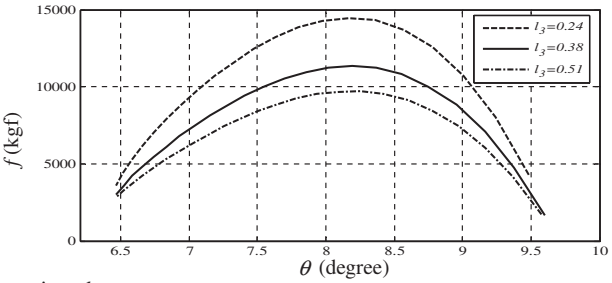

(c) for various l_3

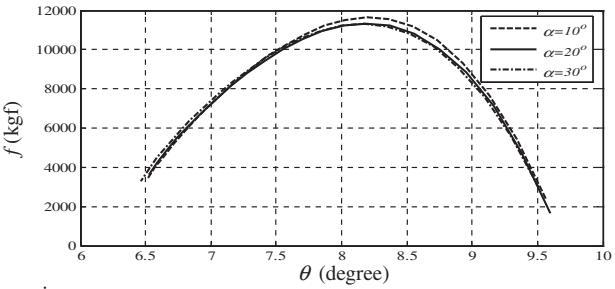

(d) for various α

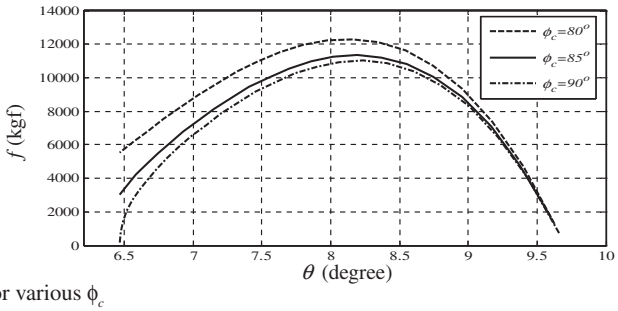

(e) for various ϕ_c

Fig. 8. Force exerted by clamping hydraulic cylinder F_D versus angle of rotation θ for various parameters l_1, l_2, l_3, α and ϕ_c, (a) for various l_1, (b) for various l_2, (c) for various l_3, (d) for various α, and (e) for various ϕ_c.

influences the maximal stroke of the moving platen and is limited by the distance between the tie bars. For $\theta = 90°$, as displayed in Fig. 3, the following relationship is obtained;

$$b_{\max} = H_c - C_B - G_B, \tag{27}$$

where H_c is the distance between Point O and CL; C_B is the outer radius of pin joint B and G_B is the distance between the outer edge of pin joint B and CL.

To increase the opening stroke, b should be set as close as possible to b_{max}. The values a/b, c/b and d/b are defined as l_1, l_2 and l_3, respectively, and the performance of the mechanism for various values of l_1, l_2, l_3, α and ϕ_c is examined. Fig. 8(a)–(d), and (e) describe the effect of key parameters l_1, l_2, l_3 α and ϕ_c on the input force f of the clamping hydraulic cylinder, respectively. BP increases with l_1, as shown in Fig. 8(a). This fact enables the toggle mechanism to overcome the BP, because the mechanical advantage increases rapidly as the mold approaches complete closure. Fig. 8(b) and (c) reveal that the effects of l_2 and l_3 on the maximum input force are greater than those of other parameters. Smaller l_2 and l_3 correspond to the need for a greater input force to overcome the BP. Conversely, the parameter α is not strongly correlated with the maximal input force, as presented in Fig. 8(d). Fig. 8(e) shows that the input forces that correspond to $\phi_c = 90°$ and $\phi_c = 85°$ have the same maximal values. However, $\phi_c \geqslant 90°$ must be averted to prevent a 'dead lock' condition, in which the toggle mechanism cannot easily open the mold. At $\phi_c \geqslant 85°$, the toggle mechanism generates sufficient MA to yield the required clamping force. Thus, $90° > \phi_c > 85°$ constrains the optimal clamping mechanism. High l_1, l_2 and l_3 ratios reduce the maximal input force provided by the clamping hydraulic cylinder.

Fig. 9 plots the speed of the moving platen as a function of angle θ for various values of l_1, based on the assumption that the angular speed of $Crank\ O$ is 1 rad/s and the maximal mold-opening stroke is constant. However, increasing l_1 reduces the initial speed of mold-closing, and causes the platen to move rapidly. However, it also increases the initial angle of mold-closing.

Fig. 10(a)–(d) plot the ratio K_v of the speed of slider A to that of D as a function of the angle of rotation θ of $Crank\ O$ for various values of l_2, l_3, α, and ϕ_c, respectively. These figures, for a mold-opening stroke of 440 mm, indicate that large l_2 and l_3 coupled with a proper α can generate a smooth K_v profile. Fig. 10(a) demonstrates that the K_v profile will increase the mold-closing process for various values of l_2. Fig. 10(b) shows that the K_v profile is sensitive to small l_3, and so succeeding values should be avoided to ensure smooth motion of the moving platen. Fig. 10(c) indicates that α substantially affects the initial speed of mold-closing, especially when it exceeds 30°. Furthermore, Fig. 10(d) reveals that ϕ_c has a relatively weak effect on the K_v profile. Analytical results reveal that a change in l_2 or l_3 parameters affects the curvature of K_v.

Fig. 11 plots the mold-opening stroke as a function angle θ; a larger l_1 corresponds to a longer mold-opening stroke. Eq. (7) demonstrates that when the mold-opening stroke increases, the ratio K_d of the stroke of the mold-opening to that of the clamping cylinder also increases. Restated, a smaller K_d corresponds to a longer clamping hydraulic cylinder stroke.

Fig. 12(a)–(d) display the K_d profiles versus mold-opening stroke for various values of parameters l_2, l_3, α, and ϕ_c, respectively. Reducing l_2 or l_3 can reduce the machine dimensions, by reducing the strokes of the clamping hydraulic cylinder. Also, the K_d value varies with the mold-opening stroke, and its variation is significant, as plotted in Fig. 12(a)–(c). In particular, when the α value varies to be less than 30°, K_d increases significantly. Thus the parameters l_2, l_3, α strongly affect the K_d value, while ϕ_c has little effect, as seen in Fig. 12(d).

In summary, the results in Figs. 8–12 show that a large l_1 can significantly improve the performance of a toggle mechanism, but increases the length of the machine. Additionally, a high l_2 yields favorable K_v and K_d curvatures, but increases the need for a large input force from the clamping hydraulic cylinder, such that the force amplification ratio is low. The l_1

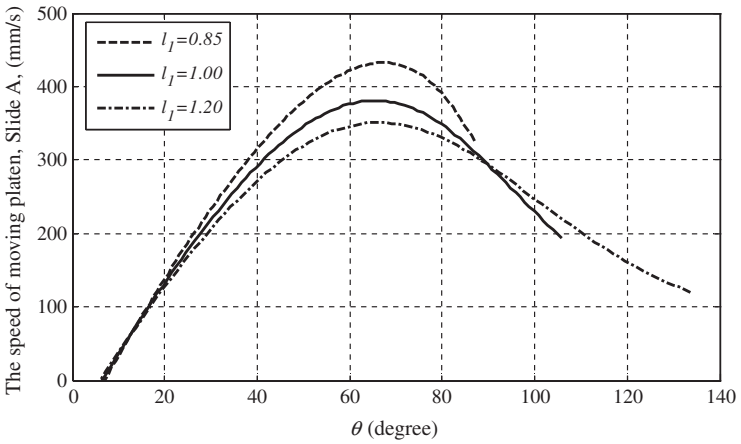

Fig. 9. Speed of moving platen as a function of θ for various l_1.

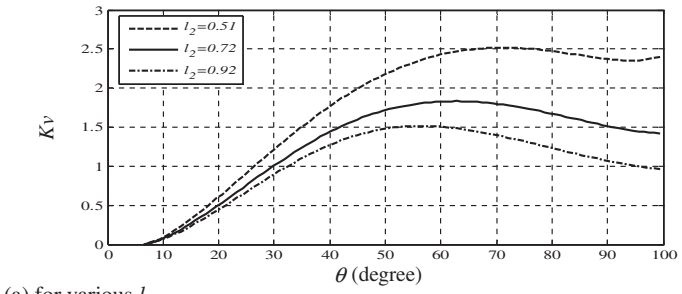

(a) for various l_2

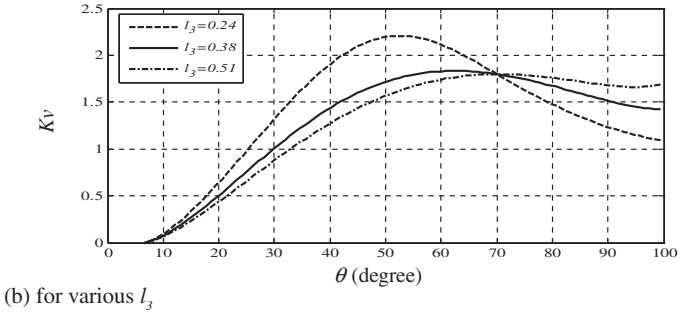

(b) for various l_3

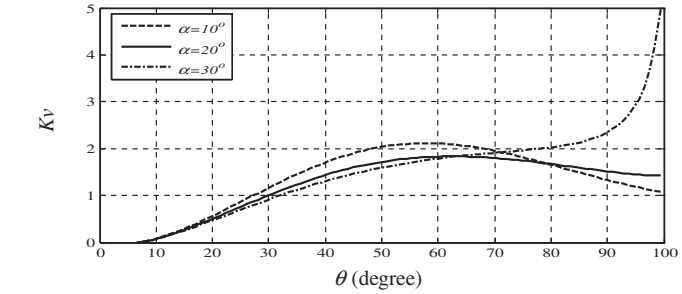

(c) for various α

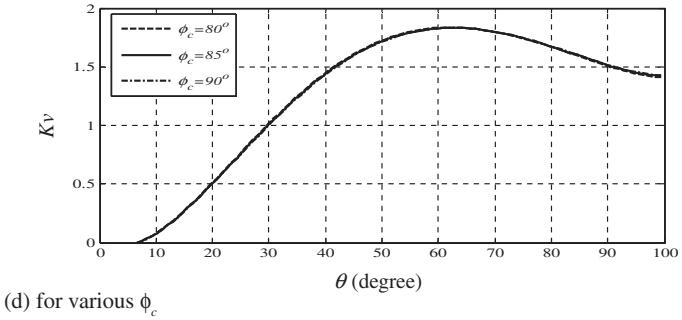

(d) for various ϕ_c

Fig. 10. Speed ratio *Kv* versus angle of rotation θ for parameters l_2, l_3, α and ϕ_c, (a) for various l_2, (b) for various l_3, (c) for various α, and (d) for various ϕ_c.

parameter is suggested to be large and the α angle is about 20° to ensure a smooth K_v curve and a high amplification ratio. The K_d value is suggested to exceed 1, and ϕ_c is approximately 85° when the force amplification ratio and the K_d value are considered.

7. Genetic algorithm approach for optimizing design parameters

In this section, the GA [12,13] is applied to optimize the values of the five main parameters l_1, l_2, l_3, α, and ϕ_c. Genetic algorithms produces a new generation of possible solutions for a given problem in each cycle. In the first phase, an initial population, describing representatives of the potential solution, is created to initiate the search process. The elements of the population are encoded into bit-strings, called chromosomes. The performance of the strings, often called fitness, is then

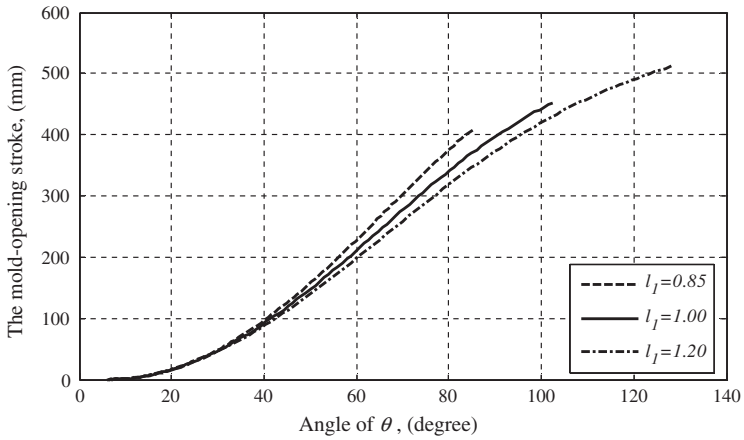

Fig. 11. Mold-opening stroke versus θ for various l_1.

evaluated with the help of some functions, representing the constraints of the problem. Depending on the fitness of the chromosomes, they are selected for a subsequent genetic manipulation process. It should be noted that the selection process is mainly responsible for assuring survival of the best-fit individuals. After selection of the population strings, the genetic manipulation process consisting of two steps is carried out. In the first step, the crossover operation that recombines the bits (genes) of each two selected strings (chromosomes) is executed. The second step in the genetic manipulation process is termed mutation, where the bits at one or more randomly selected positions of the chromosomes are altered. The mutation process helps to overcome trapping at local maxima. The offsprings produced by the genetic manipulation process are the next population to be evaluated. Before executing the GA process, some specifications must be decided for the GA, i.e. population size, maximum generation number, crossover probability, mutation probability, the fitness function, the range of each parameter, etc. Note that the setting specifications must be reasonable, because good initial parameters and specifications dramatically speed up the convergence. In this paper, we assign the searching range of each parameter based on experiences. The procedure is as follows.

- Step 1. *Input the machine specifications and constraints.* The specifications, given in Table 1, include the mold-opening stroke A_m, the offset h of slider A, the maximal clamping force F, the radii R_O, R_A, R_B, R_C and R_D of the pin joints, the friction coefficient μ, the tie bar length L, the cross-sectional area A, and the elastic modulus E. The constraints on F_M and ϕ_o are specified as ranges, based on reasonable dimensions of the clamping hydraulic cylinder and the initial speed of the mold-closing. The ranges are determined empirically, and their constraining equations are generally given as follows.

$$F_{M\min} \leqslant F_M \leqslant F_{M\max}, \tag{28}$$

$$\phi_{\min} \leqslant \phi_o \leqslant \phi_{\max}, \tag{29}$$

  where F_M ranges from 19 to 23 and ϕ_c ranges from 18° to 24°.
- Step 2. *Generate an initial population and evaluate the goal function.* A binary population is generated randomly. It must be transferred into real numbers before the goal function is calculated. In this work, the population size is 40 and the number of generations is 10. All phenotypes of the population are used to calculate the goal function given as follows.

$$GF = Min\left[\left(\frac{Kv_{\max}}{Kv_{\min}} - R^*_{Kv}\right)^2 + (K_d - K^*_d)^2\right], \tag{30}$$

  where Kv_{max} and Kv_{min} are calculated using Eq. (8) and represent the local maximum and the local minimum in the Kv curve, respectively. The ratio Kv_{max}/Kv_{min} represents the smoothness of the motion of the platen. K^*_d is the desired value of the stroke ratio K_d in Eq. (7) and R^*_{Kv} is the desired ratio of Kv_{max} to Kv_{min}. An R^*_{Kv} value of close to 1 indicates the smooth motion of the moving platen. The goal function in Eq. (30) minimizes the errors in the stroke ratio and speed ratio with respect from the respective desired values; their weightings are equal. The goal function is an important performance index or life index, and determines whether the chromosome can continue to exist or is eliminated in the evolutionary process.
- Step 3. *Perform coding and decoding.* Binary encoding is the most common, mainly because first works about GA used this type of encoding. In binary encoding every chromosome is a string of bits, 0 or 1. Binary encoding gives many possible chromosomes even with a small number of alleles. On the other hand, this encoding is often not natural for many problems and sometimes corrections must be made after crossover and/or mutation. When the GA is used to solve the

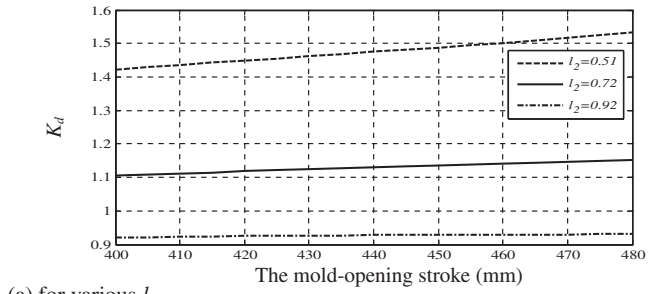

(a) for various l_2

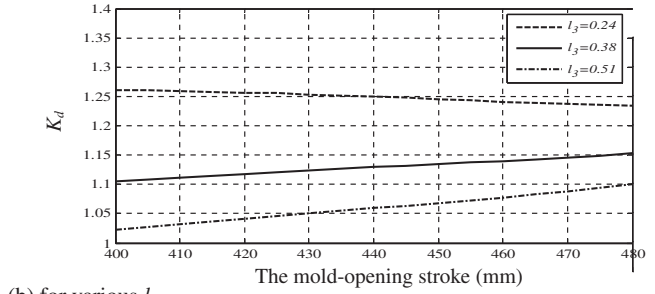

(b) for various l_3

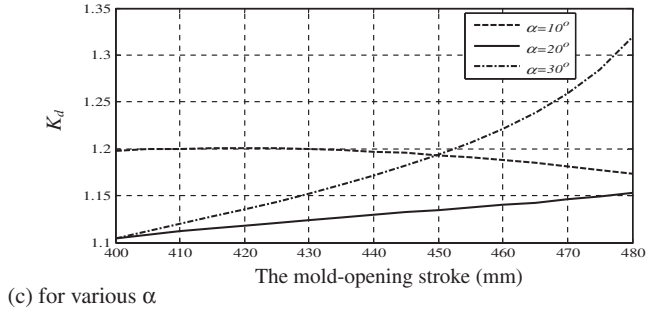

(c) for various α

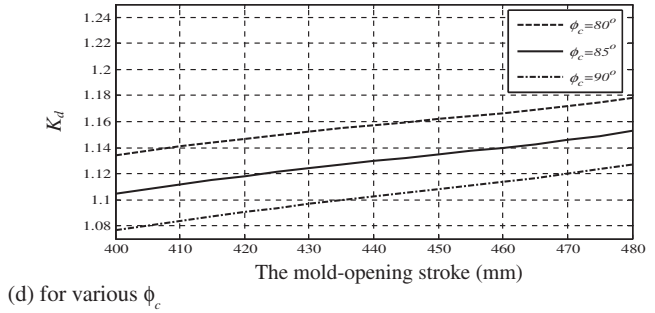

(d) for various ϕ_c

Fig. 12. Ratio K_d of stroke mold-opening to that of clamping hydraulic cylinder versus mold-opening stroke for parameters various values of l_2, l_3, α *and* ϕ_c, (a) for various l_2, (b) for various l_3, (c) for various α, and (d) for various ϕ_c.

Table 1
List of specifications of design parameters.

R_O	34 mm	h	66 mm	Hc	355 mm
R_A	34 mm	F	200 ton	E	21,000 kgf/mm^2
R_B	34 mm	L	2330 mm	μ	0.2
R_C	17 mm	A	5674.5 mm^2	SC	$GF \leqslant 10^{-4}$
R_D	17 mm	C_B	57 mm	–	–
A_m	470 mm	G_B	5 mm	–	–

SC: Stop condition.

problem, each searching range must be coded as a binary string to enable the reproduction, crossover and mutation of chromosomes, and then the binary string is decoded as a real number to calculate the goal function. In this work, the length of every chromosome is 50.

- Step 4. *Perform reproduction.* In the GA, roulette wheel selection is applied as the method of reproduction. The chromosome is reproduced in the next generation based on the value of its goal function. A greater value of the goal function corresponds to a larger area of the roulette wheel associated with the chromosome, and a greater probability of reproduction of the chromosome.
- Step 5. *Perform crossover.* These two chromosomes, which are randomly selected from the reproduced chromosomes, exchange their genes with each other. In this study, double-point crossover is adopted, and the initial crossover rate is set to 0.8. When the crossover rate increases to 0.95, the values of the goal functions remain constant in the subsequent 20 generations. The crossover rate becomes 0.8 when the value of the goal function is changing.
- Step 6. *Perform mutation.* Mutation is a process by which a binary population is randomly and the characteristic, which is the selected binary population, is randomly changed from 0 to 1, or from 1 to 0. In a manner similar to the crossover rate, the mutation rate is set to 0.05 initially. The rate rises to 0.1 after the values of the goal functions have not changed for 20 generations, and are returned to 0.05 when the goal function value change. This process is intended to yield a local solution.
- Step 7. *Define the stopping rule.* Since the GA follows the uninterrupted competition and propagation unless a stopping rule is activated, a stopping rule terminates the calculation when the goal function is less than 10^{-4}. If the stopping rule is not satisfied, repeat Step 3.

8. Case studies and comparisons

From the derived equations, including those for the friction in each pin joint, the motion performance is defined as follows; the ratio K_d of the mold-opening stroke to the stroke of the clamping hydraulic cylinder, and the ratio Kv_{max}/Kv_{min} of the maximal speed to the minimal speed of the moving platen are used in the goal function, as in Eq. (29). Furthermore, the force amplification ratio F_M of the clamping force F to the maximal input force f_{max}, and the angle ϕ_o between *Link d* and the motion line of slider D, as presented in Eqs. (28) and (29), respectively, are constraints on the optimal design of the toggle mechanism.

Applying the GA, the mechanism is relatively simple and fast. Moreover, the design of the injection-molding machines with various clamping forces is efficient and all of these machines perform identically. This innovative design approach satisfies the requirements of actual industrial applications.

The optimal solutions in Table 2 can be obtained from the design parameters specified in Table 1, and are compared with those of the primary mechanism. $Kv_{max}/Kv_{min} = 1.14$ is closer to the ideal value of $R^*_{Kv} = 1.15$ than is 1.21 obtained with the primary design; the ratio of the mold-opening stroke to the stroke of the clamping hydraulic cylinder is also closer to the ideal value. The K_d value in the primary design is only 0.987: the stroke of the clamping hydraulic cylinder is longer than that of the mold opening, so the efficiency is poor. The optimal design by GA increases the K_d value to 1.007, and improves the efficiency. Additionally, the force amplification ratio is substantially promoted.

The two curves in Fig. 13(a) plot the *MA* values that correspond to friction coefficients of 0 and 0.2. If the friction coefficient is 0.2, then the instantaneous *MA* value must be 58.6 at the moment of full mold closure. In contrast, the instantaneous MA value under the friction-free condition is 49,188, which is clearly unreasonable. Accordingly, the friction coefficient must be considered in establishing a mathematical model for designing toggle mechanism. Fig. 13(b) and (c) compare the forces of the clamping hydraulic cylinder, and the ratios of speed and stroke of mold-opening to those of clamping hydraulic cylinder for both the optimization by GA and the primary design. The optimal force of the clamping hydraulic cylinder is smaller, and the optimal speed ratio Kv is larger than the corresponding values for the primary design. The stroke ratios of the mold-opening to the clamping hydraulic cylinder in the two cases are close to each other.

Table 2
Optimal solutions for toggle clamping mechanism.

Items		Feasible domains or desirable value	Primary design	Optimal solution
b (mm)		–	293	293
The designed parameters (mm)	l_1	1.0–1.2	1.150	1.195
	l_2	0.5–0.9	0.800	0.752
	l_3	0.3–0.5	0.464	0.495
	α	10°–30°	17.43°	16.33°
	ϕ_c	70°–90°	83.87°	85.80°
Kv_{max}/Kv_{min}		$R^*_{Kv} = 1.15$	1.21	1.14
Stroke ratio of the mold-opening to the clamping hydraulic cylinder		$K^*_d = 1$	0.987	1.007
The initial angle of mold-closing		18–24°	20.6°	23.6°
Force amplification ratio F_M		19–23	19.93	20.40

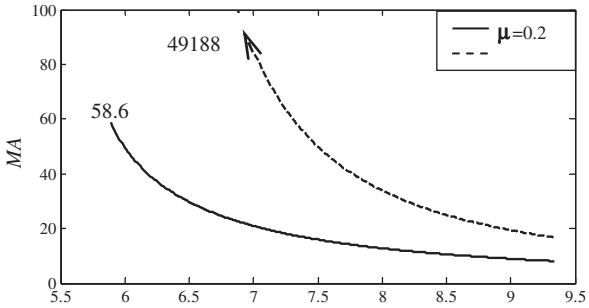

(a) mechanical advantage

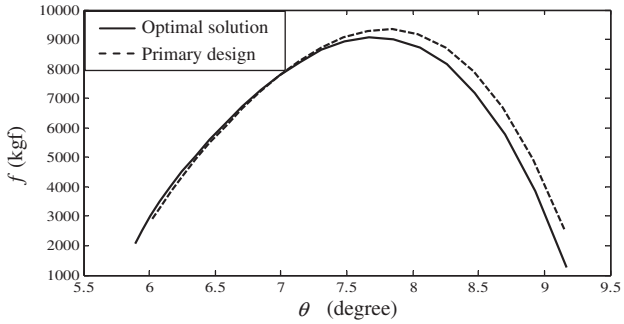

(b) force F_D exerted byclamping hydraulic cylinder

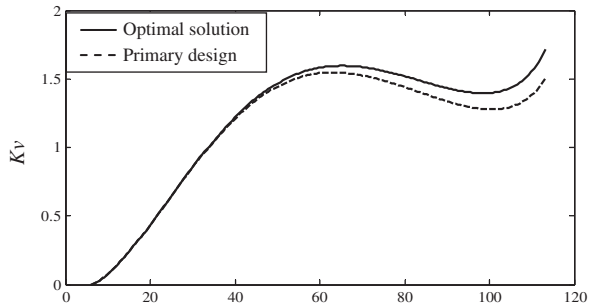

(c) speed ratio *Kv*

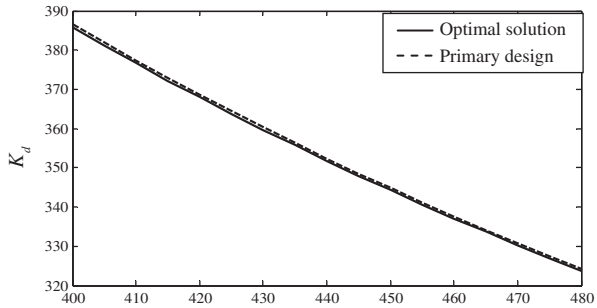

(d) stroke of clamping hydraulic cylinder versus mold-opening stroke

Fig. 13. Comparisons between optimal solution and primary design. (a) Mechanical advantage, (b) force F_D exerted by clamping hydraulic cylinder, (c) speed ratio *Kv*, and (d) stroke of clamping hydraulic cylinder versus mold-opening stroke.

9. Conclusions

In this work, key design parameters, including the stroke of the clamping hydraulic cylinder, the initial speed of mold-closing, the ratio of force amplification, and the speed profile of the moving platen are considered to elucidate the

performance of a five-point double-toggle clamping mechanism. The GA approach is adopted to obtain the optimal solution based on these key design parameters. The following conclusions are drawn.

(1) The l_2 and l_3 parameters significantly influence the values of f_{max}, Kv, and K_d. A high l_2 value yields favorable Kv and K_d curvatures, but increases the need for a large input force to be exerted by the clamping hydraulic cylinder, and thus for a low force amplification ratio.
(2) A large l_1 value can significantly improve the performance of the toggle mechanism, but it increases the length of the machine. The l_1 parameter should be large and the α angle should be approximately 20° to yield a smooth Kv curve and a high amplification ratio.
(3) The K_d value should exceed one, and ϕ_c should be around 85° when the force amplification ratio and the K_d value are taken into account.
(4) When the GA method is applied, Kv_{max}/Kv_{min} and the ratio of the stroke of the mold-opening to the stroke of the clamping hydraulic cylinder are closer to the ideal values than those obtained with the primary design, and the small force of the clamping hydraulic cylinder saves input energy. Accordingly, the GA method is a good design tool, which improves the performance of a five-point double-toggle clamping mechanism.

Acknowledgements

The authors would like to thank Ted Knoy for his editorial assistance.

References

[1] P. Burton, Kinematics and Dynamics of Planar Machinery, Prentice Hall, Englewood Cliffs, NJ, 1979.
[2] F.P. Beer, E.R. Johnston, Vector Mechanics for Engineers – Statics, McGraw Hill, New York, 1984.
[3] G.H. Martin, Kinematics and Dynamics of Machines, McGraw Hill, New York, 1982.
[4] C.E. Wilson, J.P. Sadler, Kinematics and Dynamics of Machinery, Harper Collins College Publishers, 1993.
[5] W.Y. Lin, M.H. Kuo, Investigation of the friction effect at pin joints for the five-point double-toggle clamping mechanisms of injection molding machines, Int. J. Mech. Sci. 45 (2003) 913–1927.
[6] W.Y. Lin, C.L. Shen, K.M. Hsiao, A case study of the five-point double-toggle mould clamping mechanism, Proc. Inst. Mech. Eng. C- J. Mech. 220 (2006) 527–535.
[7] W.Y. Lin, K.M. Hsiao, Study on improvements of the five-point double-toggle mould clamping mechanism, Proc. Inst. Mech. Eng. C- J. Mech. 218 (2004) 761–774.
[8] R.F. Fung, C.C. Hwang, C.S. Huang, W.P. Chen, Inverse dynamics of a toggle mechanism, Comput. Struct. 63 (1997) 91–99.
[9] R.F. Fung, C.C. Hwang, C.S. Huang, Kinematic and sensitivity analyses of a new type toggle mechanism, Jpn. Soc. Mech. Eng. Ser. C 40 (1997) 360–365.
[10] A. Mostofi, Toggle mechanisms: dynamics and energy dissipation, Mech. Mach. Theory 20 (1985) 83–93.
[11] R.F. Fung, J.W. Wu, D.S. Chen, A variable structure control toggle mechanism driven by a linear synchronous motor with joint coulomb friction, J. Sound Vib. 247 (2001) 741–753.
[12] J.H. Holland, Adaptation in Natural and Artificial Systems, The University of Michigan Press, Ann Arbor, MI, 1975.
[13] D.E. Goldberg, Genetic Algorithms in Search, Optimization and Machine Learning, Addison-Wesley, Reading, MA, 1989.